

Theoretical research on terahertz wave generation from planar waveguide by optimized cascaded difference frequency generation

Zhongyang Li(李忠洋), Jia Zhao(赵佳), Wenkai Liu(刘文锴), Qingfeng Hu(胡青峰), Yongjun Li(李永军), Binzhe Jiao(焦彬哲), Pibin Bing(邴丕彬), Hongtao Zhang(张红涛), Lian Tan(谭联), and Jianquan Yao(姚建铨)

Citation: Chin. Phys. B, 2021, 30 (**2**): 024209. DOI: 10.1088/1674-1056/abc3b7
Journal homepage: http://cpb.iphy.ac.cn; http://iopscience.iop.org/cpb

What follows is a list of articles you may be interested in

High-gain and low-distortion Brillouin amplification based on pump multi-frequency intensity modulation

Li-Wen Sheng(盛立文), De-Xin Ba(巴德欣), Zhi-Wei Lv(吕志伟)
Chin. Phys. B, 2019, 28 (**2**): 024212. DOI: 10.1088/1674-1056/28/2/024212

Guiding properties of proton-implanted Nd^{3+}-doped phosphate glass waveguides

Qi-Feng Zhu(朱其峰), Yue Wang(王玥), Jian-Ping Shen(沈建平), Hai-Tao Guo(郭海涛), Chun-Xiao Liu(刘春晓)
Chin. Phys. B, 2018, 27 (**5**): 054218. DOI: 10.1088/1674-1056/27/5/054218

Phase estimation of phase shifts in two arms for an SU(1,1) interferometer with coherent and squeezed vacuum states

Qian-Kun Gong(龚乾坤), Dong Li(李栋), Chun-Hua Yuan(袁春华), Ze-Yu Qu(区泽宇), Wei-Ping Zhang(张卫平)
Chin. Phys. B, 2017, 26 (**9**): 094205. DOI: 10.1088/1674-1056/26/9/094205

Planar waveguides in neodymium-doped calcium niobium gallium garnet crystals produced by proton implantation

Chun-Xiao Liu(刘春晓), Meng Chen(陈梦), Li-Li Fu(付丽丽), Rui-Lin Zheng(郑锐林), Hai-Tao Guo(郭海涛), Zhi-Guang Zhou(周志广), Wei-Nan Li(李玮楠), She-Bao Lin(林社宝), Wei Wei(韦玮)
Chin. Phys. B, 2016, 25 (**4**): 044211. DOI: 10.1088/1674-1056/25/4/044211

Optical planar waveguides in Yb^{3+}-doped phosphate glasses produced by He^{+} ion implantation

Liu Chun-Xiao, Li Wei-Nan, Wei Wei, Peng Bo
Chin. Phys. B, 2012, 21 (**7**): 074211. DOI: 10.1088/1674-1056/21/7/074211

Theoretical research on terahertz wave generation from planar waveguide by optimized cascaded difference frequency generation*

Zhongyang Li(李忠洋)[1,†], Jia Zhao(赵佳)[1], Wenkai Liu(刘文锴)[2], Qingfeng Hu(胡青峰)[2], Yongjun Li(李永军)[1], Binzhe Jiao(焦彬哲)[1], Pibin Bing(邴丕彬)[1], Hongtao Zhang(张红涛)[1], Lian Tan(谭联)[1], and Jianquan Yao(姚建铨)[3]

[1] *College of Electric Power, North China University of Water Resources and Electric Power, Zhengzhou* 450045, *China*
[2] *College of Surveying and Geo-informatics, North China University of Water Resources and Electric Power, Zhengzhou* 450045, *China*
[3] *College of Precision Instrument and Opto-electronics Engineering, Institute of Laser and Opto-electronics, Tianjin University, Tianjin* 300072, *China*

(Received 15 August 2020; revised manuscript received 14 September 2020; accepted manuscript online 22 October 2020)

A novel scheme for high-efficiency terahertz (THz) wave generation based on optimized cascaded difference frequency generation (OCDFG) with planar waveguide is presented. The phase mismatches of each-order cascaded difference frequency generation (CDFG) are modulated by changing the thickness of the waveguide, resulting in a decrement of phase mismatches in cascaded Stokes processes and an increment of phase mismatches in cascaded anti-Stokes processes simultaneously. The modulated phase mismatches enhance the cascaded Stokes processes and suppress the cascaded anti-Stokes processes simultaneously, yielding energy conversion efficiencies over 25% from optical wave to THz wave at 100 K.

Keywords: terahertz wave generation, optimized cascaded difference frequency generation, planar waveguide

PACS: 42.65.Yj, 42.65.Dr, 42.65.Ky **DOI:** 10.1088/1674-1056/abc3b7

1. Introduction

Terahertz (THz) waves have extensive scientific and technological applications, such as spectroscopy, biomedical engineering, communication, non-destructive inspection, and imaging fields.[1–5] However, intense and inexpensive THz wave sources are still difficult to realize, which hinders the development of THz wave applications. In order to achieve intense THz waves from optical waves by frequency conversion technology, a single optical photon must produce several THz photons due to the large ratio between optical and THz frequencies. Cascaded difference frequency generation (CDFG) is a promising method to generate numerous THz photons from a single pump photon.[6–10] CDFG involves cascaded Stokes processes in which THz photons are generated and cascaded anti-Stokes processes in which THz photons are consumed. The more cascaded Stokes processes are stimulated, the more THz photons are generated. However, the phase mismatches of the cascaded Stokes processes increase rapidly with the cascading orders, which restricts the energy transfer from pump wave to THz wave.[10] Therefore, how to reduce the phase mismatches of cascaded Stokes processes and enlarge the phase mismatches of cascaded anti-Stokes processes simultaneously is of vital importance.

In this work, we propose a novel scheme that paves the way toward high-efficiency THz wave generation by optimized cascaded difference frequency generation (OCDFG) with a planar waveguide. The modulation of THz wave effective refractive index by changing the thickness of planar waveguide can lead to the phase mismatches of cascaded Stokes processes equalling zero one by one from the first-order Stokes process to high-order Stokes processes. At the same time, the phase mismatches of cascaded anti-Stokes processes are enlarged. Compared with reported CDFG, more pump photons are transferred to high-order cascaded Stokes processes by OCDFG, yielding an optical-to-THz energy conversion efficiency of 25.8% by OCDFG with 3000 MW/cm^2 pump intensity at 100 K.

2. Theoretical model

The guiding mode can exist in the planar waveguide structures, such as TE and TM guiding modes for the THz wave.[11] The phase-matching condition of the first-order Stokes process in the waveguide is expressed as

$$\frac{n_{\rm p}}{\lambda_{\rm p}} - \frac{n_{\rm s}}{\lambda_{\rm s}} = \frac{n_{\rm eff,THz}}{\lambda_{\rm T}}, \tag{1}$$

where n and λ represent refractive index and wavelength, the subscripts p, s, and T represent pump wave, signal wave, and THz wave. $n_{\rm eff,THz}$ is the effective refractive index of the fundamental TM-mode THz wave. The relationship between effective refractive index $n_{\rm eff,THz}$ and waveguide thickness t is obtained from the following equation:[11]

$$\frac{t}{\lambda_{\rm T}} = \frac{1}{\pi\sqrt{n_{\rm T}^2 - n_{\rm eff,THz}^2}} \tan^{-1}\left(n_{\rm T}\sqrt{\frac{n_{\rm eff,THz}^2 - 1}{n_{\rm T}^2 - n_{\rm eff,THz}^2}}\right). \tag{2}$$

*Project supported by the National Natural Science Foundation of China (Grant Nos. 61735010, 31671580, and 61601183), Natural Science Foundation of Henan Province, China (Grant No. 162300410190), and Program for Science & Technology Innovation Talents in Universities of Henan Province, China (Grant No. 18HASTIT023).

†Corresponding author. E-mail: thzwave@163.com

© 2021 Chinese Physical Society and IOP Publishing Ltd

The effective refractive index $n_{\mathrm{eff,THz}}$ of the fundamental TM-mode THz wave varies with the thickness of the waveguide.

According to the principle of OCDFG, the incident pump wave (ω_0) interacts with the first-order Stokes wave (ω_1) to generate THz photon (ω_{T}). Given that the phase-matching condition of the first-order Stokes process is satisfied, the amplified first-order Stokes wave ($\omega_1 = \omega_0 - \omega_{\mathrm{T}}$) acts as a new high-frequency pump wave to generate second-order Stokes wave ($\omega_2 = \omega_1 - \omega_{\mathrm{T}}$) and THz wave. As long as the phase-matching OCDFG processes continue, a series of cascaded Stokes waves with frequencies of ω_m spectrally separated by the THz frequency ω_{T} are generated. The integer m denotes the m-th order cascaded optical waves. Meanwhile, the generated THz wave interacts with the incident pump wave by sum-frequency generation (SFG), generating the first-order anti-Stokes wave ω_{-1} ($\omega_{-1} = \omega_0 + \omega_{\mathrm{T}}$). If this process continues, a series of cascaded anti-Stokes waves ω_{-m} are generated. The coupled wave equation of OCDFG can be derived from the common nonlinear optical three-wave interaction equations

$$\frac{\mathrm{d}E_{\mathrm{T}}}{\mathrm{d}z} = -\frac{\alpha_{\mathrm{T}}}{2}E_{\mathrm{T}} + \mathrm{j}\,\kappa_{\mathrm{T}}\sum_{-\infty}^{+\infty} E_m E_{m+1}^{*}\,\mathrm{e}^{\mathrm{j}\Delta k_m z}, \tag{3}$$

$$\frac{\mathrm{d}E_m}{\mathrm{d}z} = -\frac{\alpha_m}{2}E_m + \mathrm{j}\,\kappa_m\left[E_{m-1}E_{\mathrm{T}}^{*}\,\mathrm{e}^{\mathrm{j}\Delta k_{m-1}z} + E_{m+1}E_{\mathrm{T}}\,\mathrm{e}^{-\mathrm{j}\Delta k_m z}\right], \tag{4}$$

$$\kappa_m = \frac{\Omega_m d_{\mathrm{eff}}}{c n_m}, \tag{5}$$

$$\kappa_{\mathrm{T}} = \frac{\Omega_{\mathrm{T}} d_{\mathrm{eff}}}{c n_{\mathrm{T}}}, \tag{6}$$

$$\Delta k_m = k_m - k_{m+1} - k_{\mathrm{eff,THz}}, \tag{7}$$

$$I = \frac{1}{2}nc\varepsilon_0\left|E\right|^2, \tag{8}$$

$$\eta\left(z\right) = \frac{n_{\mathrm{eff,THz}}\left(\omega_{\mathrm{T}}\right)\left|E_{\mathrm{T}}(\omega_{\mathrm{T}},z)\right|^2}{\sum n\left(\omega_m\right)\left|E_m(\omega_m,0)\right|^2}, \tag{9}$$

where E denotes the electric field amplitude, α denotes the absorption coefficient, κ is the coupling coefficient, Ω is the angular frequency, k is the wave vector in the waveguide, Δk is the phase mismatch, d_{eff} is the nonlinear coefficient, c is the speed of light in vacuum, I is the power density, ε_0 is vacuum dielectric constant. $\eta\left(z\right)$ is the energy conversion efficiency along with the waveguide length z. The first term of the right-hand side of Eq. (3) indicates the THz wave absorption, and the second term represents the sum of the THz wave intensity generated by the interaction between ω_m and ω_{m+1} during the OCDFG. The first term of the right-hand side of Eq. (4) indicates the absorption of cascaded optical waves, the second term represents the enhancement of ω_m by the interaction between ω_{m-1} and ω_{T}, and the third term represents the consumption of ω_m by the interaction between ω_{m+1} and ω_{T}.

3. Calculations

In this section, we take MgO:$LiNbO_3$ planar waveguide as an example. The input pump frequency ω_{p} is 291.76 THz, and ω_{T} is 0.5 THz. The absorption coefficients of the cascaded optical waves and terahertz waves in MgO:$LiNbO_3$ waveguide are 0 cm^{-1} and 2.10 cm^{-1} at 100 K, respectively.[12] The nonlinear coefficient of MgO:$LiNbO_3$ at 291.76 THz is 336 pm/V.[7] The theoretical values of the refractive index of MgO:$LiNbO_3$ in the infrared region[13] and THz region[12] are calculated using the wavelength- and temperature-dependent Sellmeier equations, respectively. The laser damage threshold of MgO:$LiNbO_3$ with the pulse duration of 100 ps is $\sim$ 10 GW/cm^2.[14] The frequency range of cascaded optical waves is set from 100.26 THz to 500.26 THz.

According to Eq. (7), the phase mismatch of mth-order CDFG changes with the effective refractive index $n_{\mathrm{eff,THz}}$, so the planar waveguide thickness t can modulate the phase mismatches of cascaded Stokes processes and cascaded anti-Stokes processes. In this section, we analyze the enhancement of the cascaded Stokes processes and suppression of the cascaded anti-Stokes processes through varying the thickness of the planar waveguide.

3.1. Planar waveguide with a nonlinearly changing thickness

When each-order Δk_m equals zero, the required planar waveguide thickness t is shown by the red curve in Fig. 1(a). It can be seen that in cascaded Stokes frequencies, the waveguide thickness $t$decreases at first and then increases with the cascading Stokes orders, while in the cascaded anti-Stokes frequencies, the waveguide thickness t monotonously increases with the cascading anti-Stokes orders. If the waveguide thickness t is designed to vary with the change of the red curve in the cascaded Stokes frequencies from 291.76 THz to 100.26 THz, the phase mismatch Δk_m in cascaded Stokes processes is equal to zero one by one from the first-order Stokes process to high-order Stokes processes. Simultaneously, the phase mismatches $|\Delta k_m|$ in cascaded anti-Stokes processes substantially increase, as shown in Fig. 1(b). The schematic diagram of the thickness variation of the waveguide is shown in the inset of Fig. 1(a), where L is the waveguide length, and w is the waveguide width. The waveguide thickness changes along with the length from t_1 to t_2.

THz wave intensities and the evolutions of cascaded optical spectra with a nonlinearly changing thickness waveguide are calculated according to Eqs. (3) and (4) and shown in Fig. 2. In Fig. 2(a), with pump intensity $I_{\mathrm{p}} = I_{\mathrm{s}} = 1$ GW/cm^2, THz wave intensities increase rapidly and reach the maximum value of 0.328 GW/cm^2 at 11.4 mm, and then decrease fast. In Fig. 2(b) with $I_{\mathrm{p}} = I_{\mathrm{s}} = 3$ GW/cm^2, THz wave intensities increase continuously and reach the maximum value of

1.549 GW/cm^2 at 6.9 mm. It can be seen from Fig. 2(a) that in the initial stage, THz wave intensities increase slowly. For 4 mm $< z <$ 11.4 mm, THz wave intensities increase fast as the diffusion range of the cascaded Stokes frequencies rapidly increases. For $z >$ 11.4 mm, the diffusion range of cascaded anti-Stokes frequencies is gradually larger than that of cascaded Stokes frequencies, so the THz wave intensities decrease. In Fig. 2(b), THz wave intensities show a monotonously upward trend for 0 mm $< z <$ 6.9 mm, and the diffusion range of cascaded Stokes frequencies is obviously larger than that of cascaded anti-Stokes frequencies. Compared with the energy conversion efficiency of 16.4% in Fig. 2(a), the energy conversion efficiency of 25.8% in Fig. 2(b) are greatly improved. Moreover, the diffusion ranges of cascaded Stokes frequencies in Fig. 2(c) is smaller than those in Fig. 2(d), and the diffusion ranges of cascaded anti-Stokes frequencies in Fig. 2(c) is larger than those in Fig. 2(d). Higher pump intensities produce wider diffusion ranges of cascaded Stokes frequencies and narrower diffusion ranges of cascaded anti-Stokes frequencies, resulting in higher THz wave intensities and energy conversion efficiencies. It can be observed from Fig. 2(d) that the diffusion ranges and the intensities of cascaded Stokes waves are larger than those of cascaded anti-Stokes waves. The above results demonstrate that the cascaded Stokes processes are significantly enhanced, and the cascaded anti-Stokes processes are effectively suppressed by using the planar waveguide with nonlinearly changing thickness.

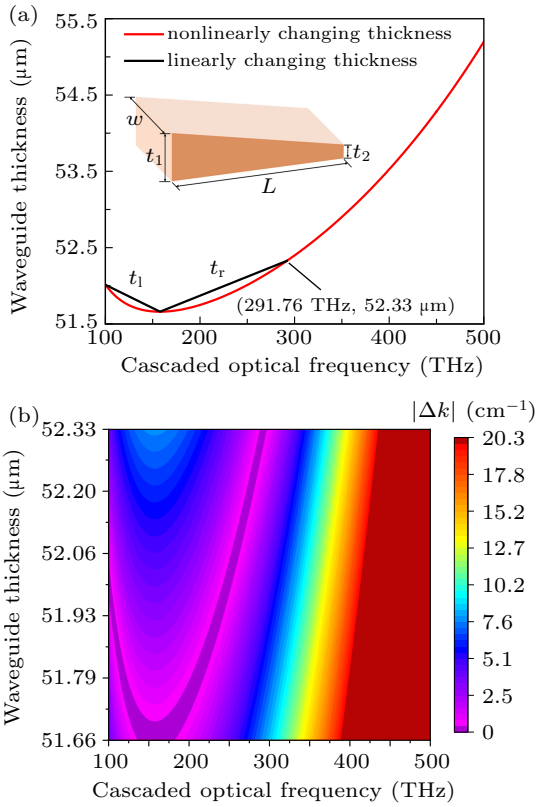


Fig. 1. (a) The waveguide thickness versus the cascaded optical frequency when Δk_m is equal to 0. Inset: schematic diagram of the planar waveguide with changing thickness. (b) The nonlinearly changing thickness and normalized $|\Delta k_m|$ versus the cascaded optical frequency.

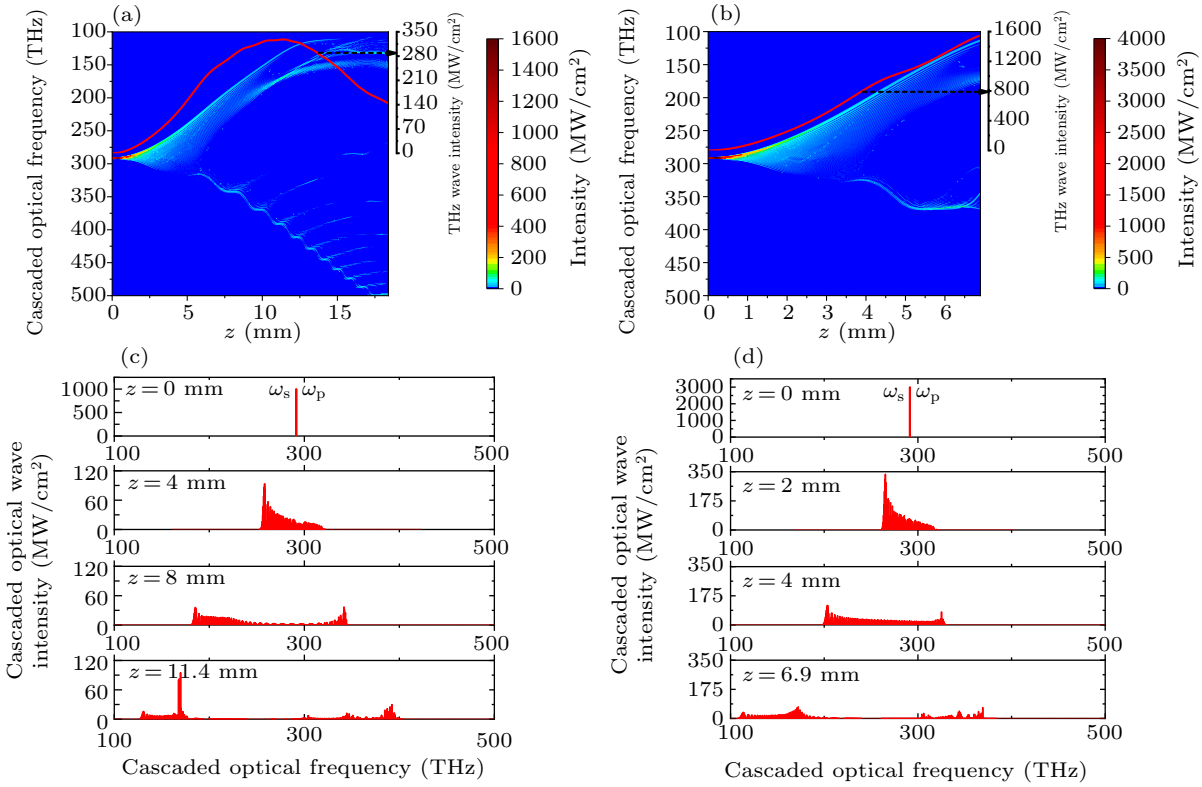


Fig. 2. THz wave intensities and optical spectra with nonlinearly changing thickness waveguide. The red curves in (a) and (b) represent the variation of the THz wave intensity, and the dashed-line arrow indicates the right longitudinal axis. (a) $I_p = I_s = 1$ GW/cm^2. (b) $I_p = I_s =$ 3 GW/cm^2. (c) Optical spectra corresponding to (a). (d) Optical spectra corresponding to (b).

3.2. Planar waveguide with a constant thickness

In this part, we analyze THz wave generations from traditional CDFG with a constant thickness MgO:LiNbO$_3$ planar waveguide. THz wave intensities and the evolutions of cascaded optical spectra with a constant thickness waveguide are shown in Fig. 3. In Fig. 3(a) with $I_p = I_s = 1$ GW/cm^2, THz wave intensities increase slowly and reach the maximum value of 107.1 MW/cm^2 at $z = 5.6$ mm, and in Fig. 3(b) with $I_p = I_s = 3$ GW/cm^2, THz wave intensities increase continuously and reach the maximum value of 475.8 MW/cm^2 at 4.0 mm. Compared with energy conversion efficiencies of 16.4% in Fig. 2(a) and 25.8% in Fig. 2(b), energy conversion efficiencies of 5.4% in Fig. 3(a) and 7.9% in Fig. 3(b) are greatly suppressed. It can be seen from Fig. 3(c) that the cascaded Stokes frequencies and the cascaded anti-Stokes frequencies at each waveguide length only diffuse to a very small frequency range. It can be observed from Fig. 3(d) that in the range from $z = 0$ mm to $z = 1.5$ mm, the cascaded Stokes frequencies and the cascaded anti-Stokes frequencies diffuse slowly, and most of the pump energy is still concentrated near the pump frequency. For 1.5 mm $< z <$ 3 mm, the intensities of cascaded Stokes waves are obviously higher than those of cascaded anti-Stokes waves. For 3 mm $< z <$ 4 mm, the generation rate of THz photon is enhanced as the cascaded Stokes frequencies rapidly diffuse to higher cascading orders. The diffusion ranges of cascaded optical frequencies in Figs. 3(c)–3(d) are substantially smaller than those in Figs. 2(c)–2(d). Since the waveguide thickness remains constant, both the phase mismatches Δk_m in cascaded Stokes processes and cascaded anti-Stokes processes increase with the cascading orders. The cascaded anti-Stokes processes consume large numbers of generated THz photons, which suppresses the cascaded Stokes processes, resulting in a decrease of THz wave intensities.

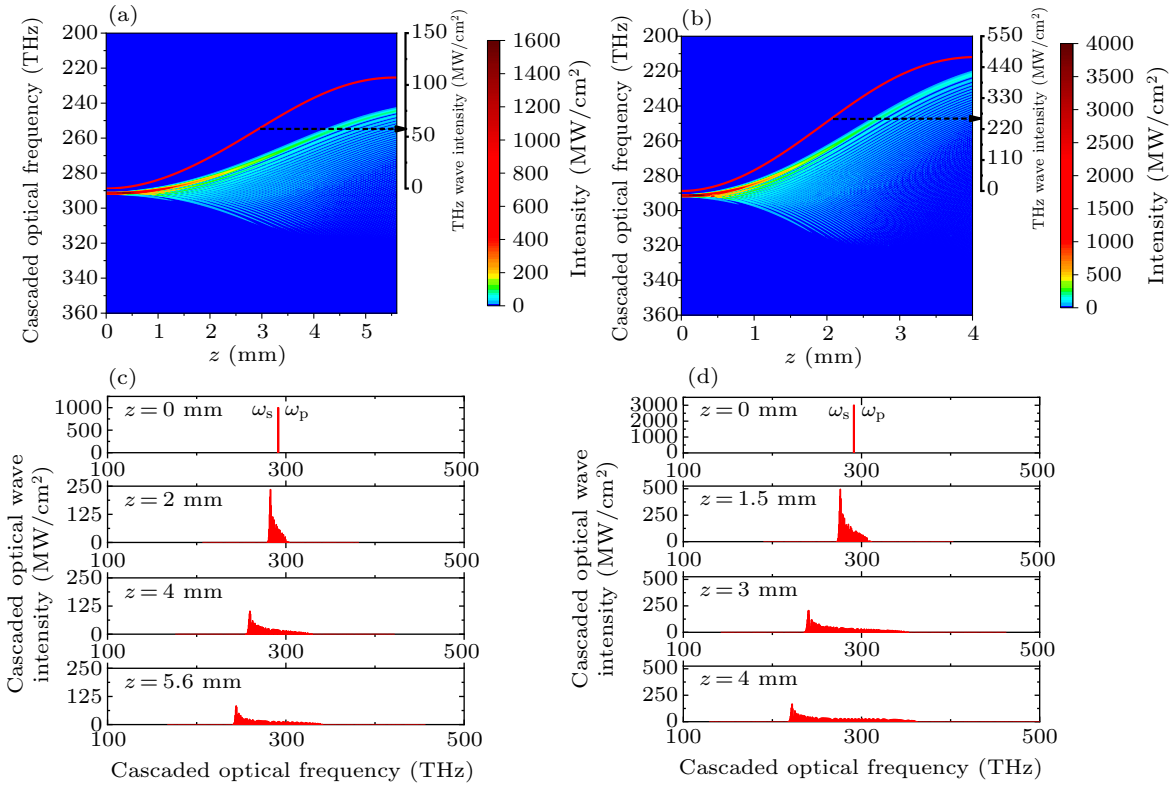


Fig. 3. THz wave intensities and optical spectra with constant thickness waveguide. The red curves in (a) and (b) represent the variation of the THz wave intensity, and the dashed-line arrow indicates the right longitudinal axis. (a) $I_p = I_s = 1$ GW/cm^2. (b) $I_p = I_s = 3$ GW/cm^2. (c) Optical spectra corresponding to (a). (d) Optical spectra corresponding to (b).

3.3. Planar waveguide with a linearly changing thickness

In this part, we propose a planar waveguide with a linearly changing thickness, as shown in Fig. 1(a) with the black curve. The black curve is divided into two parts t_r and t_l. t_r changes from the thickness corresponding to the first-order phase-matching cascaded Stokes process to the minimum thickness of the red curve in Fig. 1(a), and t_l changes from the minimum thickness to the thickness corresponding to the highest-order phase-matching cascaded Stokes process. t_r and t_l are expressed as

$$t_r = 0.004968 \times \left(f_p - f_T \times \left(\frac{N \times z}{L} \right) \right) + 50.87658, \quad (10)$$

$$t_l = -0.0061 \times \left(f_p - f_T \times \left(\frac{N \times z}{L} \right) \right) + 52.62258. \quad (11)$$

The unit of t_r and t_l is μm. f_p and f_T represent the frequency of pump wave and THz wave, respectively, and the unit of f_p and f_T is THz. N is the number of cascaded Stokes frequency, and L is the optimal waveguide length.

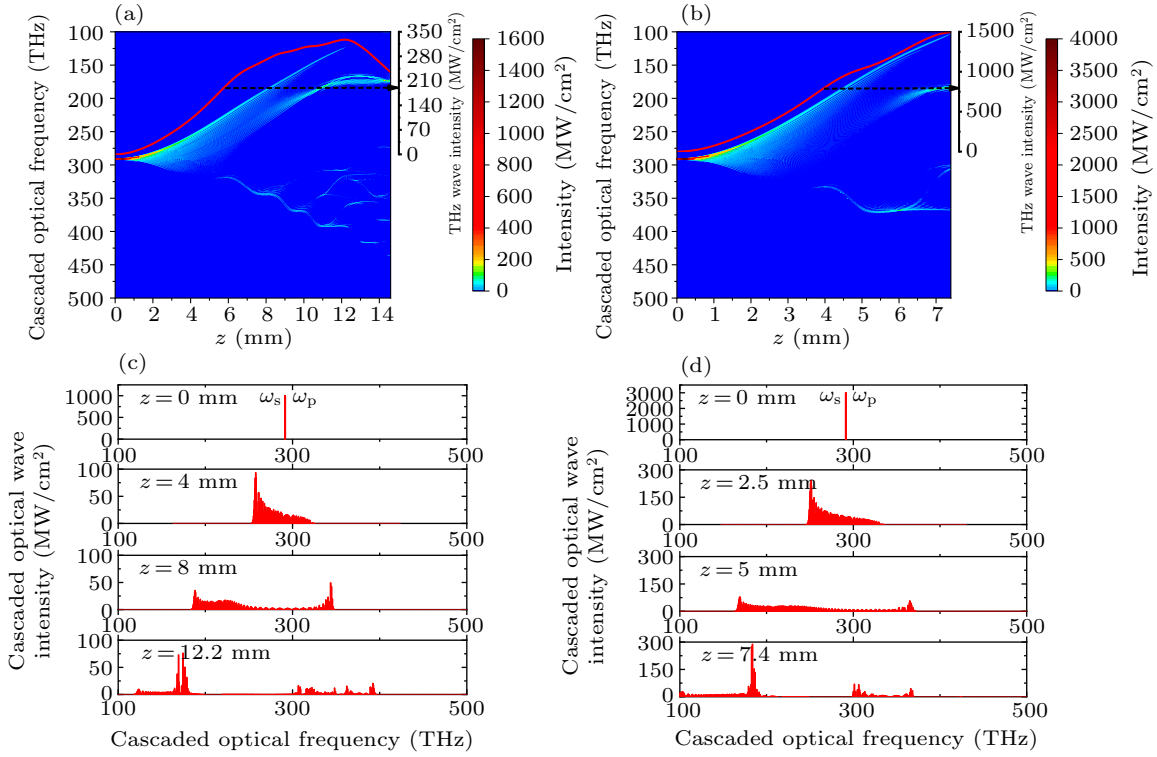


Fig. 4. THz wave intensities and optical spectra with linearly changing thickness waveguide. The red curves in (a) and (b) represent the variation of the THz wave intensity, and the dashed-line arrow indicates the right longitudinal axis. (a) $I_p = I_s = 1$ GW/cm^2. (b) $I_p = I_s = 3$ GW/cm^2. (c) Optical spectra corresponding to (a). (d) Optical spectra corresponding to (b).

THz wave intensities and the evolutions of cascaded optical spectra with a linearly changing thickness waveguide are shown in Fig. 4. In Fig. 4(a) with $I_p = I_s = 1$ GW/cm^2, THz wave intensities increase slowly and reach the maximum value of 327.5 MW/cm^2 at $z = 12.2$ mm, and in Fig. 3(b) with $I_p = I_s = 3$ GW/cm^2, THz wave intensities increase monotonously and reach the maximum value of 1.495 GW/cm^2 at $z = 7.4$ mm. Compared with energy conversion efficiencies of 16.4% in Fig. 2(a) and 25.8% in Fig. 2(b), energy conversion efficiencies of 16.38% in Fig. 3(a) and 24.92% in Fig. 3(b) are slightly decreased. The diffusion ranges and the intensities of cascaded optical waves are broadly similar to those in Fig. 2. As shown in Fig. 1(a), the differences between the red curve and the black curve at the same frequency are minimal, which ensures that the phase mismatches Δk_m with a linearly changing thickness waveguide are close to those with a nonlinearly changing thickness waveguide. The planar waveguide with a linearly changing thickness is convenient to manufacture and shows a result analogous to that with a nonlinearly changing thickness.

4. Discussion

Compared with the maximum energy conversion efficiency of 7.9% from traditional CDFG with a constant thickness waveguide shown in Fig. 3(b), the maximum energy conversion efficiency is enhanced by 3.27 and 3.15 times by OCDFG from the planar waveguide with a nonlinearly changing thickness and a linearly changing thickness, respectively. Compared with the reported theoretical work with an energy efficiency of 8% by CDFG with PPLN at 77 K,[15] the energy efficiency of 25.8% in this work is attributed to the decrease of phase mismatches in cascaded Stokes processes and increase of phase mismatches in cascaded anti-Stokes processes simultaneously. OCDFG proposed in this work can efficiently generate THz frequencies in the range of 0.1–3 THz with low THz wave absorption coefficients. The scheme can be applied to other planar waveguides, such as GaAs, GaP.

In practice, experimental setups mainly consist of a planar waveguide and two pump lasers with frequencies separated by the generated THz frequency. The two pump lasers can be realized by a compact broadband Q-switched Yb:YAG laser[16] or by a KTP-OPO at the degeneracy point.[17] The planar waveguide with a linearly changing thickness is convenient to manufacture, while the planar waveguide with a nonlinearly changing thickness is difficult to manufacture. The existing manufacturing technology for two pump lasers and planar waveguide with a linearly changing thickness makes high-efficiency THz wave generation by OCDFG practically feasible.

5. Conclusion

We propose a novel scheme for high-efficiency THz wave generation based on OCDFG with a planar waveguide. By designing the planar waveguide with a nonlinearly or linearly changing thickness, the phase mismatches of cascaded Stokes processes equal zero one by one from the first-order Stokes

process to high-order Stokes processes, while the phase mismatches of cascaded anti-Stokes processes fundamentally increase. As a result, the modulated phase mismatches enhance the cascaded Stokes processes and suppress the cascaded anti-Stokes processes simultaneously, yielding energy conversion efficiencies over 25% at 100 K.

References

[1] Tonouchi M 2007 *Nat. Photon.* **1** 97
[2] Jepsen P U, Cooke D G and Koch M 2011 *Laser Photonics Rev.* **5** 124
[3] Zhang X C, Shkurinov A and Zhang Y 2017 *Nat. Photon.* **11** 16
[4] Murate K and Kawase K 2018 *J. Appl. Phys.* **124** 160901
[5] Yoshida S, Hirori H, Tachizaki T, Yoshioka K, Arashida Y, Wang Z-H, Sanari Y, Takeuchi O, Kanemitsu Y and Shigekawa H 2019 *ACS Photon.* **6** 1356
[6] Liu P, Xu D, Yu H, Zhang H, Li Z, Zhong K, Wang Y and Yao J Q 2013 *J. Lightw. Technol.* **31** 2508
[7] Ravi K, Schimpf D N and Kärtner F X 2016 *Opt. Express* **24** 25582
[8] Saito K, Tanabe T and Oyama Y 2015 *J. Opt. Soc. Am. B* **32** 617
[9] Li Z Y, Yao J Q, Xu D G, Zhong K, Wang J L and Bing P B 2011 *Chin. Phys. B* **20** 054207
[10] Li Z Y, Sun X Q, Li Y J, Yuan B, Zhang H T, Bing P B, Wang Z and Yao J Q 2020 *Opt. Lasers Eng.* **128** 106035
[11] Saito K, Tanabe T and Oyama Y 2012 *Opt. Express* **20** 26082
[12] Pálfalvi L, Hebling J, Kuhl J, Péterá and Polgár K 2005 *J. Appl. Phys.* **97** 123505
[13] Jundt D H 1997 *Opt. Lett.* **22** 1553
[14] Carbajo S 2015 *Stanford Linear Accelerator Center* (Personal Communication)
[15] Ravi K, Hemmer M, Cirmi G, Reichert F, Schimpf D N, Mücke O D and K?rtner F X 2016 *Opt. Lett.* **41** 3806
[16] Zhao P, Ragam S, Ding Y J and Zotova I B 2012 *Conference on Lasers & Electro-optics, IEEE*, San Jose, California United States p. QF3G.2
[17] Zhong K, Yao J, Xu D, Wang Z, Li Z, Zhang H and Wang P 2010 *Opt. Commun.* **283** 3520